Bilirubin kinetics in intact rats and isolated perfused liver. Evidence for hepatic deconjugation of bilirubin glucuronides.

J Gollan, … , V Licko, R Schmid

J Clin Invest. 1981;67(4):1003-1015. https://doi.org/10.1172/JCI110111.

Research Article

Most previous compartmental models describing bilirubin transport and metabolism in the liver have been validated solely by analysis of the plasma disappearance of radiolabeled bilirubin in human subjects. We now have determined the transport kinetics of a bilirubin tracer pulse by analysis of plasma, liver, and bile radioactivity data from 30 intact rats. Plasma [3H]bilirubin disappearance was best described by the sum of three exponentials, and a six-compartment model, derived by simulation analysis, was necessary and adequate to describe all experimental data. Examination of the injected radiolabeled bilirubin by extraction with hexadecyltrimethylammonium bromide and thin-layer chromatography revealed that 6.6% (mean) of the original pigment had been degraded to labeled nonbilirubin derivatives during preparation of the tracer dose. This material exhibited a significantly longer half-life (mean 50.6 min) of the plasma terminal exponential than that of authentic radiobilirubin (20.6 min). In isolated perfused rat liver, the kinetics of [3H]bilirubin in perfusate and bile readily fitted the proposed model. Compatibility of the model with the data obtained, both in the isolated liver and in vivo, required that a fraction of bilirubin conjugated in the liver be deconjugated and returned to the plasma. Deconjugation of bilirubin glucuronides was evaluated directly by infusion of bilirubin monoglucuronides, containing 14C in the glucuronosyl group, into rats with an external bile fistula. Since metabolic degradation of hydrolyzed […]

Bilirubin Kinetics in Intact Rats and Isolated Perfused Liver

EVIDENCE FOR HEPATIC DECONJUGATION OF BILIRUBIN GLUCURONIDES

JOHN GOLLAN, LYDIA HAMMAKER, VOJTECH LIČKO, and RUDI SCHMID, *Department of Medicine, the Liver Center, and Cardiovascular Research Institute, University of California School of Medicine, San Francisco, California 94143*

ABSTRACT Most previous compartmental models describing bilirubin transport and metabolism in the liver have been validated solely by analysis of the plasma disappearance of radiolabeled bilirubin in human subjects. We now have determined the transport kinetics of a bilirubin tracer pulse by analysis of plasma, liver, and bile radioactivity data from 30 intact rats. Plasma [^{3}H]bilirubin disappearance was best described by the sum of three exponentials, and a six-compartment model, derived by simulation analysis, was necessary and adequate to describe all experimental data. Examination of the injected radiolabeled bilirubin by extraction with hexadecyltrimethylammonium bromide and thin-layer chromatography revealed that 6.6% (mean) of the original pigment had been degraded to labeled nonbilirubin derivatives during preparation of the tracer dose. This material exhibited a significantly longer half-life (mean 50.6 min) of the plasma terminal exponential than that of authentic radiobilirubin (20.6 min). In isolated perfused rat liver, the kinetics of [^{3}H]bilirubin in perfusate and bile readily fitted the proposed model. Compatibility of the model with the data obtained, both in the isolated liver and in vivo, required that a fraction of bilirubin conjugated in the liver be deconjugated and returned to the plasma.

Deconjugation of bilirubin glucuronides was evaluated directly by infusion of bilirubin monoglucuronides, containing ^{14}C in the glucuronosyl group, into rats with an external bile fistula. Since metabolic degradation of hydrolyzed ^{14}C-labeled glucuronic acid yields $^{14}CO_2$, this was measured in expired air. Whereas 86% of the administered labeled pigment was recovered in bile, 7% of the label appeared in $^{14}CO_2$. These findings directly validate a portion of the proposed kinetic model and suggest that hepatic deconjugation of a small fraction of bilirubin glucuronides is a physiological event. Deconjugation may also account, at least in part, for the presence of increased concentrations of unconjugated bilirubin in the plasma of patients with cholestasis.

INTRODUCTION

Kinetic analysis and mathematical modeling of plasma bilirubin-IXα (bilirubin)[1] disappearance curves have provided important insight into the complex processes of hepatic bilirubin transport and metabolism (2). Although in early studies large doses of unlabeled pigment had been used (3), the subsequent availability of isotopically labeled bilirubin of high specific activity (4, 5) permitted experiments to be performed under more physiological conditions using tracer doses of the pigment. These investigations (2, 6–11), which provided a measure of the rates of hepatic bilirubin clearance and bilirubin production, resulted in the formulation of a three-compartment model that adequately described the metabolism of unconjugated bilirubin. In addition, more complex models have been proposed to accommodate the bilirubin fractions derived from turnover of hepatic heme and hemoproteins (12–14). These models have been used to interpret data derived from plasma radiobilirubin disappearance studies in various human disorders associated with unconjugated hyperbilirubinemia (13, 15–19).

This paper was presented in part in November 1979 at the Annual Meeting of the American Association for the Study of Liver Disease (1).

Address reprint requests to Dr. Gollan.

Received for publication 31 March 1980 and in revised form 5 November 1980.

[1] *Abbreviations used in this paper*: bilirubin, bilirubin-IXα; BMG, bilirubin monoglucuronide; BDG, bilirubin diglucuronide: TLC, thin-layer chromatography.

All of these investigations were carried out in humans and hence validation of the proposed compartmental models was restricted to analysis of data obtained from a single compartment, e.g., plasma radiobilirubin disappearance. Indeed, in only two subjects were data obtained from bile, namely in an individual with an external bile fistula (8) and in a patient with Gilbert's syndrome in whom bile was collected from the duodenum (13). To minimize the assumptions required in formulating a model and thus to reduce inherent ambiguities and uncertainties, it is desirable to verify experimentally as many of the proposed compartments as possible. Although use of experimental animals permits serial sampling of bile and liver, animal studies with radiolabeled bilirubin have been carried out only in intact rats to define plasma disappearance (20, 21) and in isolated rat liver perfused with an erythrocyte-containing medium to determine bilirubin kinetics in perfusate and bile (22). With rose bengal dye, on the other hand, experiments in rats have been reported in which plasma, liver, and intestinal contents were sampled serially (23).

In the present study a new and more sensitive procedure for quantitation of plasma bilirubin has been used, obviating the use of the Weber-Schalm solvent-partition method (24) that has been widely adopted (8, 22, 25) despite its documented inaccuracies (8, 26–28). Using this procedure we have examined the hepatic transport kinetics of radiobilirubin in 30 intact rats and developed a compartmental model that described all experimental data obtained from plasma, liver, and bile. The proposed model, which was validated by kinetic studies in isolated rat liver perfused with a heme-free fluorocarbon medium, differs from existing models in predicting that a fraction of bilirubin glucuronides in the liver undergoes deconjugation with return of unconjugated bilirubin so formed to the plasma. This prediction was verified experimentally by measurement of $^{14}CO_2$ production in rats infused with bilirubin [^{14}C]monoglucuronide.

METHODS

Chemicals and radiolabeled pigments

Bilirubin consisting of at least 94% IXα isomer was obtained from Koch-Light Lab., Ltd. (Colnbrook, Buckinghamshire, U. K.) or Porphyrin Products (Logan, Utah) and recrystallized before use (29). [^{3}H]Bilirubin (sp act 43 μCi/μmol) prepared biosynthetically (4) from the bile of rats injected with δ-amino [3,5-^{3}H]levulinic acid (1.2 Ci/mmol, New England Nuclear, Boston, Mass.) was stored *in vacuo* in the dark and recrystallized to constant specific activity before use. Bilirubin-IXα 1-O-acyl β-D-mono-[U-^{14}C]glucuronide (BMG) was prepared by incubating bilirubin-IXα and UDP-[U-^{14}C]glucuronic acid (231 mCi/mmol, New England Nuclear) with digitonin-activated liver microsomes from rats pretreated with phenobarbital (administered for 7 d in drinking water, 0.1% wt/vol). Details of the incubation, extraction, and chromatographic isolation of BMG have been described (30, 31). The pigment was quantitated spectrophotometrically assuming E_{450} 60 × 10^3 liter·mol^{-1}·cm^{-1} for BMG in methanol. The yield of labeled BMG was 30% and the preparation contained 90–93% authentic BMG in addition to 4% BDG and 3–6% nonradioactive unconjugated bilirubin (32). When eluted from silica gel with methanol and promptly evaporated to dryness and stored in the dark under argon at −20°C, BMG preparations were stable for at least 2 d. Immediately before injection, the BMG was dissolved directly in normal rat serum, whereas [^{3}H]bilirubin was dissolved in a small volume of 0.1 M NaOH and then added to 14 vol of rat serum. All procedures were carried out in subdued light to minimize photodegradation of pigments.

[^{3}H]*Bilirubin kinetics—intact rats*

Fed male Sprague-Dawley rats (Simonsen Laboratories, Inc., Gilroy, Calif.) weighing 375±5 g (±SEM) were used. During the experiments they were warmed by infrared lamps. The left jugular vein was cannulated with PE-10 tubing (Clay Adams Div., Becton, Dickinson & Co., Parsippany, N. J.) under ether anesthesia, and in experiments of <30 min duration light ether anesthesia was maintained throughout the study. The animals were hydrated by infusion of 5% (wt/vol) glucose in aqueous 0.15 M NaCl (1.5 ml/h) in studies lasting >5 min. A bolus of 0.05 μmol [^{3}H]bilirubin in a total volume of 0.3 ml was administered through the jugular cannula immediately after dissolving the pigment in serum. Additional experimental details relating to the collection of samples are outlined below.

Plasma disappearance. A PE-50 cannula was inserted into the left carotid artery to permit rapid collection of blood into heparinized Natelson capillary tubes (Scientific Products Inc., McGaw Park, Ill.). Plasma disappearance of [^{3}H]bilirubin was measured in 16 rats for up to 120 min after injection. Four series of experiments were performed during which six to eight blood samples of 0.2 ml were obtained at different but overlapping time intervals after injection: (*a*) at 20-s intervals from 30 to 150 s, (*b*) at 1-min intervals from 1 to 5 min, (*c*) at 5-min intervals from 5 to 30 min, and (*d*) at 10, 20, 30, 45, 60, 90, and 120 min. The capillary tubes were centrifuged and the plasma was removed for measurement of total radioactivity and unconjugated [^{3}H]bilirubin (see Analytical procedures). To ascertain that plasma bilirubin disappearance was not affected by anesthesia, [^{3}H]bilirubin was injected into four restrained rats at least 60 min after cessation of anesthesia and blood samples were obtained at the intervals outlined above.

Liver. Total radioactivity in liver was measured in 11 separate experiments at intervals ranging from 5 to 120 min after intravenous injection of [^{3}H]bilirubin. Each experiment was terminated by rapid cannulation of the portal vein and perfusion of the liver with 35 ml of ice-cold 0.154 M KCl. The liver was resected promptly and weighed (mean liver weight, 12.8±0.5 g), and a 25% (wt/vol) homogenate was prepared in 0.154 M KCl solution. Radioactivity was then determined in duplicate in 0.4-ml aliquots of homogenate and the results were calculated for total liver.

Bile. After a series of preliminary studies that had defined optimal experimental conditions, biliary excretion of [^{3}H]bilirubin was examined in a group of three rats placed in wire restraining cages following cannulation of the bile duct with a 10-cm length of PE-50. Bile was collected into tared tubes and bile flow was determined gravimetrically. After a 30-min control period, when it was ensured that bile flow was constant, [^{3}H]bilirubin was administered as an intravenous bolus. Bile was then collected continuously for 2.5-min periods over the initial 30 min, for 5-min periods over the next 30 min, and

as a single collection over the ensuing 60 min. Radioactivity was measured in a 50-μl aliquot of each bile sample.

[^3H]*Bilirubin kinetics—isolated perfused liver*

Isolated rat livers were perfused with a hemoglobin-free medium consisting of a perfluorochemical emulsion as oxygen-carrier in a Krebs-Ringer bicarbonate solution (Fluosol-43, Alpha Therapeutic Corp., Los Angeles, Calif.). In addition fraction V bovine serum albumin (1% wt/vol, Sigma Chemical Co., St. Louis, Mo.), 22.3 μM sodium taurocholate (Calbiochem-Behring Corp., American Hoechst Corp., San Diego, Calif.) and penicillin (100 U/ml) were included in the medium. This solution was thoroughly mixed, passed though a 10 μM Millipore filter (Millipore Corp., Bedford, Mass.), and the pH adjusted to 7.45 with 0.1 M $NaHCO_3$. In preliminary studies it was ascertained that the constituents of Fluosol-43 did not bind bilirubin.

The perfusion system, housed in a thermostatically controlled lucite cabinet, contained 50 ml of perfusate that was recirculated by means of a peristaltic pump (Multiperpex 2115, LKB Instruments, Bromma, Sweden). The medium was stirred in a glass reservoir and then passed in sequence through a membrane oxygenator (33) comprising 4 m of coiled Silastic tubing (0.147 cm i.d., 0.196 cm o.d., Dow-Corning Corp., Midland, Mich.), a temperature-sensitive probe connected to a thermostat (maintained at 37°C), a stainless steel filter screen (Millipore Corp.), a bubble trap and pressure gauge, and eventually the portal vein through a teflon cannula. The perfusate was oxygenated initially with a mixture of 95% O_2 and 5% CO_2 at a flow rate of 400 ml/min until just before the isolated liver was placed in the circuit, at which time 100% O_2 was introduced and continued for the rest of the experiment.

Male Sprague-Dawley rats weighing 360–380 g were used as liver donors. In general the operative technique described by Hems et al. (34) was used. Under ether anesthesia the bile duct was cannulated with PE-10 tubing. The portal vein was cannulated with a 16 gauge catheter (Angiocath, Deseret Pharmaceuticals, Sandy, Utah), the liver was flushed with 400 IU heparin (Liquaemin) in 0.8 ml 0.15 M NaCl Perfusion was commenced with an oxygenated Krebs-Henseleit Ringer bicarbonate solution (35) containing 2% (wt/vol) glucose, at about 8 ml/min. The interval between interruption of portal blood flow and commencing perfusion amounted to <40 s. The inferior vena cava was then cannulated above the diaphragm; the liver was dissected from the animal, transferred to the perfusion chamber on nylon mesh, and connected to the recirculating Fluosol-43 medium. A constant perfusion rate of 25 ml/min was maintained in all experiments, with a portal pressure of ~3 cmH_2O. To stabilize bile flow, sodium taurocholate was infused into the reservoir at a rate of 0.56 μmol/min. All perfusions were conducted in dim light to prevent photodegradation of bilirubin.

After a 30-min equilibration period, [^{3}H]bilirubin (0.05 μmol) was added as a bolus to the reservoir. Perfusate samples (0.5 ml) were removed from the reservoir at frequent intervals for 120 min. The samples were centrifuged at 27,000 *g* for 10 min to separate the fluorocarbon particles and total radioactivity was measured in aliquots of supernatant fluid. Similarly, bile collected periodically for 120 min into tared tubes was weighed and the radioactivity was determined. The volume of circulating perfusate was adjusted during the course of the experiments to replace loss caused by the removal of samples.

In preliminary experiments, the 1% (wt/vol) bovine serum albumin added to the Fluosol-43 perfusate was shown to stabilize the [^{3}H]bilirubin and prevent its oxidative degradation. The perfusate pH declined slowly from pH 7.4 to 7.25 during the 2-h experimental period. Viability of perfused livers was satisfactory at the end of the 2.5-h perfusion period as reflected by the normal appearance on electron microscopy, stable perfusate lactic dehydrogenase and transaminase activity, and normal hepatic oxygen consumption (2.6–2.9 μmol/min per g liver) (36). Bile flow decreased from 1.52±0.17 μl/min per g liver (1.02±0.06 ml/h) during the control period to 1.07±0.09 μl/min per g liver after 2-h perfusion.

Analytical procedures

Total radioactivity was measured in aliquots of whole plasma (25–50 μl) after mixing with 1 ml Soluene-350 (Packard Instrument Co., Downers Grove, Ill.), bleaching with 0.2 ml isopropyl alcohol and 0.2 ml 30% hydrogen peroxide, and adding 10 ml Dimilume (Packard Instrument Co.). Authentic unconjugated [^{3}H]bilirubin was determined in each plasma sample by the following method. Immediately after separation of the plasma, an aliquot (0.1 ml) was mixed with 0.1 ml rat plasma containing 0.04 μmol of unlabeled carrier bilirubin. After storing the mixture overnight at −20°C, it was extracted by a procedure developed by Dr. Colin Berry.[2] Water (0.8 ml) and 1.55-ml extraction mixture (chloroform/methanol, 1:2.1 vol/vol, containing hexadecyltrimethylammonium bromide [cetrimide], 5 mg/ml) were added and the solution mixed and centrifuged. The yellow organic phase was applied directly to precoated thin-layer chromatography (TLC) plates (Silica-gel 60, 5763, 0.25-mm thickness, Merck AG, Darmstadt, Germany) and developed in the dark for ~60 min with chloroform-methanol-water (10:5:1, vol/vol). In preliminary experiments it had been ascertained that in this system (R_f 0.90) and also in chloroform-acetic acid (99:1, vol/vol) (37), [^{3}H]bilirubin radioactivity migrated as a single band and cochromatographed with authentic bilirubin. The yellow bilirubin band was scraped from the plate and extracted twice with a total of 4 ml chloroform. The absorption of the supernatant fluid at 454 nm was measured and the solution then evaporated. The residue was dissolved in Soluene-350 and radioactivity was determined after preparation of the sample as described above. Specific activity of the extracted bilirubin was computed, and the total [^{3}H]bilirubin radioactivity in the original plasma sample was obtained by multiplying the specific activity by the amount of carrier added. The contribution of native unlabeled bilirubin in the plasma sample was assumed to be negligible in relation to the amount of carrier added.

An aliquot of each dose of [^{3}H]bilirubin injected into intact animals or the liver perfusion medium was analyzed by the cetrimide extraction and TLC procedure as described above. When the computed specific activity of the extracted bilirubin was multiplied by the amount of pigment in the dose plus the added carrier, the isotope content of authentic [^{3}H]bilirubin was found to be consistently lower (6.6±0.3%) than the total radioactivity of the injected dose. This difference appeared to be the result of degradation of a small fraction of the added pigment to labeled diazo-negative derivatives (4, 38), occurring during the brief period when the pigment was dissolved in 0.1 M NaOH before its addition to serum (4, 38, 39). A difference between the computed isotope in authentic [^{3}H]bilirubin and total radioactivity was found in all plasma samples collected from intact rats that had been given a tracer pulse of [^{3}H]bilirubin. This appeared to reflect the presence

[2] Personal communication.

in the administered dose of labeled degradation products coinjected with the authentic [^{3}H]bilirubin, but direct quantitation of these degradation products in the small collected plasma samples was beyond the resolution of the analytical methods available. Although it is theoretically possible that the fraction of total label in plasma that corresponded to labeled bilirubin degradation products might also have included some labeled conjugated bilirubin, none could be identified by TLC of plasma extracts.

Radioactivity was determined in aliquots of the administered dose of [^{3}H]bilirubin, plasma, liver, and bile after preparation of the samples using Soluene-350, isopropyl-alcohol, hydrogen peroxide, and Dimilume as described above. Radioactive counting was performed in a liquid scintillation spectrometer (Beckman LS-250, Beckman Instruments, Fullerton, Calif.). All samples were counted for 40,000 counts or 10 min to ensure an error in net count rate of <1%. Counting efficiency determined with a [^{3}H] toluene internal standard was used to correct counts to disintegrations per minute. All data obtained from plasma, liver, and bile were expressed as a fraction of total ^{3}H-radioactivity (disintegrations per minute) in the administered dose.

Data analysis

Preliminary kinetic profiles of the data from intact animals and isolated perfused liver were obtained by resolving the plasma (total ^{3}H-activity or ^{3}H-unconjugated bilirubin) and perfusate (total ^{3}H-activity) disappearance curves into their exponential components. The data, expressed as a fraction of dose per milliliter of plasma or perfusate, were fitted to sums of two and three exponential functions by a nonlinear least squares method, weighted by the reciprocal of the square of concentration (40). The function used took the form:

$$p(t) = \sum_{j=1}^{n} A_j \exp(-\lambda_j t), \quad (1)$$

where p denotes plasma concentration; t, time; A_j, intercept of the j-th exponential; and λ_j, decay rate coefficient of the j-th exponential.

From the parameters of the exponential fit, initial distribution volume (V) (milliliters) was computed from the equation:

$$V = \frac{1}{p(0)} = \frac{1}{\sum_{j=1}^{n} A_j}, \quad (2)$$

and the total plasma clearance rate (C, milliliters per minute) was estimated as follows:

$$C = \frac{1}{\int_0^{\infty} p(t)dt} = \frac{1}{\sum_{j=1}^{n} \frac{A_j}{\lambda_j}}. \quad (3)$$

To characterize the kinetics of hepatic bilirubin transport, a variety of models were examined. This was accomplished by testing visually the degree of fit between the experimental data and numerically integrated differential equations describing the model (achieved by adjustment of fractional transfer constants). In this search, the Euler method (41) was used, and implemented on a desk-top computer (HP 9825A Hewlett-Packard Co., Palo Alto, Calif.) interfaced with a HP 9872A plotter. In keeping with current concepts of bilirubin metabolism, four distinct pools were considered in intact rats: plasma, extravascular (intra- and extrahepatic), hepatic, and biliary. The models were examined for their ability to fit the experimentally obtained data on plasma disappearance, hepatic content, and biliary excretion of injected [^{3}H]bilirubin. The most appropriate model was selected and then tested for its ability to fit the data obtained from isolated perfused liver.

In the final stage of fitting the model to data from both intact animals and perfused liver, an objective criterion, sum of squares weighted by reciprocal variances, was employed using the HP 9825A desk-top computer. Sensitivity analysis was also performed, which delineates the degree of certainty with which each parameter was estimated with respect to the minimization of the sum of squares. The sensitivity is expressed as fractional second difference of the sum of squares when the parameter changes by 1%. The greater the sensitivity, the more confidence can be placed on the parameter and the less uncertainty is involved in its estimation.

Statistical methods.

Results are shown throughout as mean and standard errors. Student's *t* test was used to estimate significance of the differences between mean values.

Deconjugation of BMG in vivo

Because the model that fitted the experimental data suggested that a portion of bilirubin glucuronides formed in the liver was hydrolyzed, an experiment was devised to test this possibility directly. The experimental approach was based on the assumption that ^{14}C-labeled glucuronic acid hydrolyzed from bilirubin [^{14}C]monoglucuronide (prepared biosynthetically from UDP-[U-^{14}C]glucuronic acid) would be metabolized in the liver with formation of $^{14}CO_2$ and ^{14}C-labeled xylulose. The latter compound then would be further degraded in the hexose monophosphate shunt to $^{14}CO_2$ (42). Hence, for each mole of BMG hydrolyzed, between 1 and 6 mol of $^{14}CO_2$ would result. The experiments were performed in rats with external biliary drainage to exclude the possibility of intestinal deconjugation and reabsorption of ^{14}C.

The jugular vein and bile duct were cannulated in four Sprague-Dawley rats (225±5 g). The animals were placed in separate glass metabolic chambers and 5% glucose in aqueous 0.15 M NaCl was infused continuously at 1.5 ml/h. After a control period of 30 min, 0.08 μmol [^{14}C]BMG in 0.7 ml rat serum was injected intravenously as a bolus. Bile and expired $^{14}CO_2$ were collected for 20 min intervals over the 1st h and 30 min intervals for a further 3 h. Cumulative excretion of radioactivity in bile samples was determined in a liquid scintillation spectrometer (counting efficiency, 94%) and expressed as a fraction of the injected dose.

The $^{14}CO_2$ collection system was similar to that described previously (43). Air from the animal chamber, drawn under vacuum, was dried with Aquasorb (Mallinckrodt, St. Louis, Mo.), and the $^{14}CO_2$ trapped in two tubes placed in series, each containing 4 ml of ethanolamine:methoxyethanol (1:1, vol/vol). 1-ml aliquots of this solution were added to 4 ml methanol, 1 ml methoxyethanol, and 12 ml Liquiflor-toluene (New England Nuclear), and the radioactivity measured with a counting efficiency of 90%. Efficiency of the CO_2 train was 95%, as determined by the recovery of a known amount of $^{14}CO_2$ released in the animal chamber. $^{14}CO_2$ production was expressed as a percentage of the administered radioactivity. The extent of bilirubin deconjugation was calculated on the assumption that the liberated labeled glucuronic acid moiety was completely metabolized to 6 mol of $^{14}CO_2$; this yielded a minimal estimate of bilirubin glucuronide hydrolysis.

TABLE I

*Model-independent Parameters Calculated from the Plasma Disappearance Curves of [^{3}H]Bilirubin and Total ^{3}H-Radioactivity in 16 Intact Rats Following [^{3}H]Bilirubin Administration**

	Three exponential fit			Two exponential fit	
Parameters‡	Unconjugated [^{3}H]bilirubin	Total ^{3}H-radioactivity	Parameters‡	Unconjugated [^{3}H]bilirubin	Total ^{3}H-radioactivity
A_1	0.0274±0.0128	0.0430±0.0082	A'_1	0.0321±0.0029	0.0393±0.0027
λ_1	0.984±0.690	0.946±0.247	λ'_1	0.214±0.029	0.185±0.020
T_1	0.704±0.494	0.733±0.192	T'_1	3.25±0.45	3.75±0.41
A_2	0.0228±0.0062	0.0259±0.0031	A'_2	0.00446±0.00076	0.00465±0.00070
λ_2	0.158±0.034	0.123±0.013	λ'_2	0.0355±0.0024	0.0191±0.0020
T_2	4.38±0.94	5.64±0.60	T'_2	19.5±1.3	36.2±3.9
A_3	0.00374±0.00085	0.00346±0.00048	—	—	—
λ_3	0.0337±0.0027	0.0160±0.0016	—	—	—
T_3	20.6±1.7	43.3±4.3	—	—	—
V	18.5±4.9	13.8±1.7		27.4±2.2	22.8±1.4
C	3.53±0.77	2.20±0.23		3.63±0.44	2.19±0.25
Standard error	4.61×10^{-5}	1.55×10^{-4}		5.02×10^{-5}	2.65×10^{-4}

* Data fitted to sum of two or three exponentials.

‡ See section on Data analysis for definition of symbols. A_j and A'_j are expressed as a fraction of administered dose per milliliter of plasma, λ_j and λ'_j as fraction per unit time (minute^{-1}), T_j and T'_j denote the half-life of the j-th exponential (minute), V the initial distribution volume (milliliter) and C the total plasma clearance rate (milliliter per minute).

RESULTS

Experiments in intact rats

Plasma disappearance. In 16 anesthetized rats, plasma disappearance of a tracer dose of [^{3}H]bilirubin administered as an intravenous bolus and followed over a period of 120 min yielded a monotonically decreasing curve. The plasma [^{3}H]bilirubin and total radioactivity data obtained from anesthetized animals were fitted to the sum of two or three exponentials, and the initial distribution volume and plasma clearance rate were determined. In unanesthetized but restrained animals, disappearance tended to be slightly more rapid, but the difference between the curves from the two groups of animals was not statistically significant, as judged by comparison of parameters of three exponential fitting. The results shown numerically in Table I and graphically for [^{3}H]bilirubin in Fig. 1 illustrate the improved quality of the three-exponential fit compared to the two-exponential fit, for both [^{3}H]bilirubin and total radioactivity disappearance.

When plasma [^{3}H]bilirubin and total radioactivity

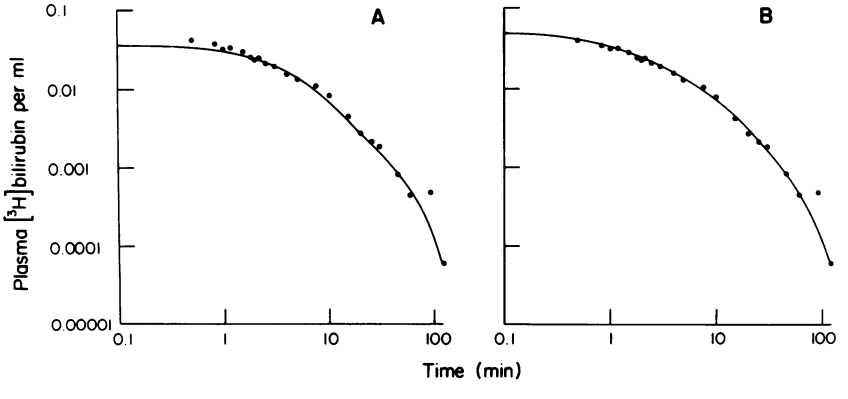

FIGURE 1 Plasma [^{3}H]bilirubin disappearance plotted as the logarithm of mean values (fraction of administered dose per milliliter) against logarithm of time (minute). The continuous lines represent the fitting of the sum of two (panel A) or three (panel B) exponentials to the data.

(including labeled degradation products) were compared, the clearance rate of the latter was considerably slower (Table I). Thus, 5 min after isotope administration, 84% (mean) of the total radioactivity in plasma was present as authentic [^{3}H]bilirubin, and this declined progressively to 67% after 30 min, 37% after 60 min and 13% after 120 min. Whereas the half-life of the first two exponentials of [^{3}H]bilirubin and of total radioactivity plasma disappearance were statistically not different, the half-life of the terminal exponential was significantly shorter for [^{3}H]bilirubin (20.6±1.7 min) than for total radioactivity (43.3±4.3 min). This observation indicates that the labeled bilirubin degradation products have a much slower plasma disappearance ($t_{1/2}$ = 50.6 ±13.6 min) than authentic [^{3}H]bilirubin.

Liver. Total radioactivity in liver was determined experimentally in 11 rats at various intervals after [^{3}H] bilirubin injection and results were calculated as a fraction of the administered dose. Because of the small amount of isotope present in the liver, separate analysis of [^{3}H]bilirubin, labeled bilirubin degradation products, and conjugated bilirubin was not possible. Because no liver samples could be obtained during the initial rapid hepatic uptake phase, the radioactivity data were fitted to only two exponentials. The values computed for A_j, expressed as a fraction of administered dose in liver; λ_j, min^{-1}; and T, min (see Data analysis section in Methods for definition of symbols) were as follows: A_1 = 0.710±0.126, A_2 = 0.073±0.012, λ_1 = 0.121±0.016, λ_2 = 0.013±0.002, T_1 = 5.75±0.76, T_2 = 53.4±8.2.

Bile. In three rats with an external bile fistula, bile flow throughout the 120 min of the experiment remained constant and averaged 1.7, 1.7, and 1.5 ml/h. With the tip of the 10-cm bile cannula placed <1 cm from the liver, the extrahepatic transit time elapsing before sample collection was ~1 min. After injection of [^{3}H]bilirubin, extraction and TLC of labeled pigments in bile showed that at least 98% of all radioactivity was present in conjugated bilirubin; labeled bilirubin degradation products could not be detected. Cumulative excretion in bile of the injected dose of [^{3}H]bilirubin was 94.0±0.2% in 2 h, which compared favorably with previously published findings (44, 45).

Compartmental model of [^{3}H]bilirubin kinetics. The compartmental model shown in Fig. 2 was found necessary and adequate to describe all the experimental data obtained from plasma, liver, and bile after injection of [^{3}H]bilirubin. This model was derived according to the following considerations. Each pool potentially could contain three radiolabeled components, namely unconjugated bilirubin, conjugated bilirubin, and bilirubin degradation products (see Legend to Fig. 2 for definition of symbols). Thus, plasma and liver pools were assumed to consist of three compartments each, although not all of these could be evaluated experimentally. Moreover, the presence of three exponentials in the plasma [^{3}H]bilirubin disappearance curve indicated that two kinetically distinct compartments were exchanging with plasma, i.e. extravascular compartment and liver (8), and hence an extravascular compartment of unconjugated bilirubin was included. Separate compartments for conjugated bilirubin in the plasma and extravascular space were not distinguished in the model. Bile was taken as a single compartment since it contains almost exclusively conjugated bilirubin (see above). To adjust for the time delay in appearance of radioactivity in bile (due to the dead-space volume of the biliary tree and bile cannula), a delay line consisting of a series of discrete compartments was inserted as is customary between the hepatic conjugated bilirubin and bile compartments. Five compartments were found to be sufficient to describe the observed delay (Fig. 2, D_1 to D_5). All exchange processes between adjacent compartments were assumed to be bidirectional, except for conjugation (r_8), the delay line (r_{10}), biliary excretion (r_9, r_{10}) of bilirubin, and the exit of labeled bilirubin degradation products from plasma (r_{13}).

The model was represented by a set of linear dif-

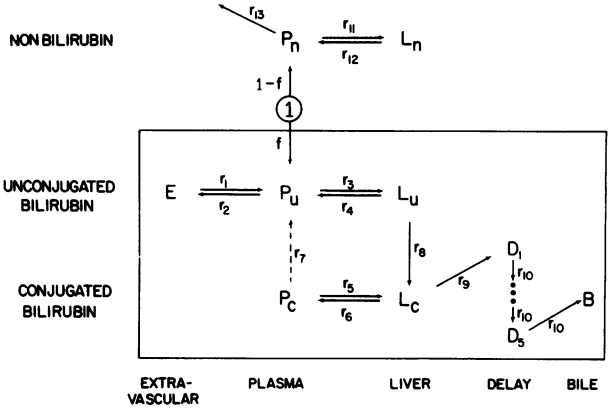

FIGURE 2 Compartmental model of [^{3}H]bilirubin metabolism in the rat. The pools are identified in appropriate columns (e.g., extravascular, plasma, etc.) and the three different radioactive components in rows. Compartments are represented by the intersection of columns with rows (e.g., P_u denotes the plasma unconjugated bilirubin compartment) and the delay line is shown as a series of five equal-sized compartments (D_1 to D_5). The symbols used to identify the compartments also stand for the fractional amount of radioactivity in those compartments. The injected dose of ^{3}H-radioactivity is identified by unity. The fraction of authentic unconjugated [^{3}H]-bilirubin in the injected dose is shown in the figure as f, and hence 1-f represents the fraction of radiolabeled bilirubin degradation products (nonbilirubin) in the dose. The movement of radiolabel between compartments is shown by arrows, and r_j identifies the fraction of radiolabel leaving the compartment per unit time (fractional rate constants). The portion of the model enclosed by the continuous line is that denoting the physiological movement of bilirubin from plasma to bile.

ferential equations that are shown in Appendix I. These equations were numerically solved for given values of the rate coefficients (r_j) as detailed in Data analysis; the results were plotted semilogarithmically in a manner that enabled direct visual comparison with the observed data. The latter consisted of (*a*) plasma [^{3}H]bilirubin concentration (P_u/V_u), (*b*) plasma concentration of radioactive bilirubin degradation products, including possibly a small fraction of labeled conjugated bilirubin ($P_n/V_n + P_c/V_c$), (*c*) hepatic radioactivity ($L_n + L_u + L_c + qE$) and (*d*) cumulative excretion of radioactivity in bile (B), where V_n and V_c represent the volume of distribution of labeled bilirubin degradation products and conjugated bilirubin, respectively, V_u is the plasma volume of distribution for [^{3}H]bilirubin, and q is the intrahepatic fraction of the extravascular pool.

Initially, deconjugation of conjugated bilirubin was not considered in the model (i.e., Fig. 2, the dashed arrow $r_7 = 0$). However, as shown in Fig. 3A, the plasma [^{3}H]bilirubin curve predicted by the model when $r_7 = 0$, was unable to simulate the observed data beyond 20 min, and overall the simulated liver and bile curves exhibited lower values than the observed data. It was evident that to achieve a decreased terminal rate of plasma unconjugated bilirubin disappearance, recycling of some conjugated bilirubin into the plasma unconjugated bilirubin compartment (P_u, Fig. 2) was necessary. This could not be achieved, however, by assuming that the process of conjugation was directly reversible because, under these circumstances, the terminal phase of the plasma curve appeared similar to that in Fig. 3A. A variety of alternative connections between compartments containing conjugated bilirubin and P_u were explored (e.g., $L_c \rightarrow P_u$), and the best results (Fig. 3B) were obtained by introducing the deconjugation pathway represented in Fig. 2 by the dashed arrow r_7.

Because the data for plasma and liver were obtained in intact rats but those for bile in bile fistula animals, duplicate simulations were carried out such that the presence or absence of an enterohepatic circulation of conjugated bilirubin was considered for plasma and liver data (i.e., insertion of an additional compartment between B and P_c; not shown in Fig. 2). It was evident that inclusion of an enterohepatic circulation in the model did not influence the fit for either the plasma or hepatic compartments during the 120-min experimental period. This is consistent with earlier direct observations that conjugated bilirubin is not reabsorbed from the intestine (46, 47).

The small proportion (6.6%) of bilirubin degradation products in the injected dose of [^{3}H]bilirubin disappeared slowly from plasma (Table I, Fig. 3) and none could be detected in bile. The ultimate mode of elimination of this fraction was not investigated, since the behaviour of these bilirubin degradation products has no relevance to the model representing physiologic bilirubin transport (shown in Fig. 2, enclosed by continuous line).

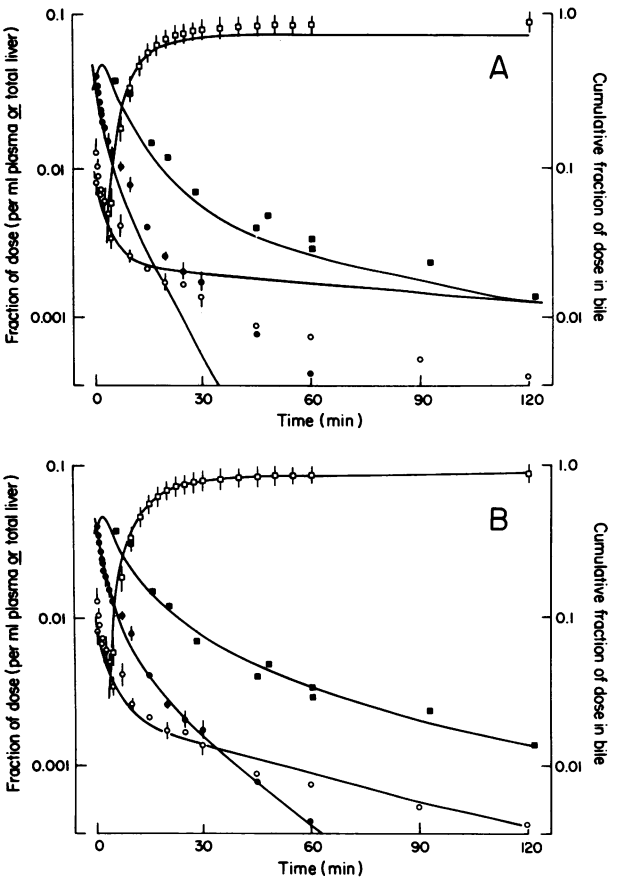

FIGURE 3 Experimental data (mean±SEM) obtained in intact rats for plasma disappearance of [^{3}H]bilirubin (●) and labeled bilirubin degradation products (○), and appearance of radioactivity in liver (■) and bile (□) following an intravenous tracer pulse of [^{3}H]bilirubin (0.05 μmol). Values for plasma and liver are expressed as a fraction of the administered dose per milliliter plasma or total liver, respectively, and radioactivity excreted in bile is shown as a cumulative fraction of the dose. Continuous lines represent the curves computed by simulation analysis from the kinetic model (Fig. 2). Fig. 3A illustrates the poor computer fit to the experimental data when the deconjugation pathway is omitted from the model ($r_7 = 0$). Fig. 3B shows the fit obtained when deconjugation (r_7) is incorporated into the model.

The fractional rate constants and distribution volumes are presented in Table II. The results indicate that net hepatic extraction is less than initial uptake (r_3), confirming previous observations in humans (8). The mean fraction $r_9/(r_8 + r_4)$ was 0.80, and thus of the bilirubin entering the hepatic pool, 20% refluxed to plasma unchanged, whereas 80% underwent conjugation. The hepatic pool of unconjugated bilirubin averaged 19% of the plasma pool [$r_3/(r_4 + r_8)$] and the mean

TABLE II

*Fractional Rate Constants and Distribution Volumes of Injected [^{3}H]Bilirubin in Intact Rats and Isolated Rat Liver**

Parameter	Intact rats	Isolated perfused liver
f	0.916 (0.6)	0.928 (5)
r_1, min^{-1}	0.198 (0.0007)	—
r_2	0.113 (0.008)	—
r_3	0.278 (0.07)	0.109 (1)
r_4	0.294 (0.002)	0.0216 (0.01)
r_5	0	0.02 (0.0005)
r_6	0.102 (0.001)	0.0551 (0.01)
r_7	0.0558 (0.0004)	0.0553 (0.002)
r_8	1.20 (0.003)	0.204 (0.01)
r_9	0.415 (0.0007)	0.374 (0.009)
r_{10}	0.570 (0.001)	0.361 (0.006)
r_{11}	0.148 (0.0008)	0.517 (0.03)
r_{12}	0.0478 (0.0008)	0.0481 (0.03)
r_{13}	0.0641 (0.002)	0
V_u, *ml*	17.0 (0.1)	18.6 (0.6)
V_c	166 (0.0003)	215 (0.0002)
V_n	7.75 (0.004)	7.78 (0.03)

* Values represent the fit of the compartmental model (Fig. 2) to the experimental data obtained in intact rats (Fig. 3B) and isolated perfused rat liver (Fig. 4). The figures shown in parentheses are sensitivities expressed as fractional second differences of the sum of squares resulting from the fractional change of the corresponding parameter by 0.01.

fraction of the total flux out of the plasma that goes to the extravascular pool ($r_2/[r_2 + r_3]$) was 29%.

Experiments in isolated perfused rat liver

Having developed a kinetic model that fitted all of the data obtained in intact rats, it was pertinent to test the validity of this model in the isolated perfused rat liver. For technical reasons, only total radioactivity was measured in perfusate and bile samples, although the injected dose of [^{3}H]bilirubin was analyzed chromatographically. In a preliminary experiment it was shown that [^{3}H]bilirubin in the administered dose (95% of total radioactivity) remained stable (coefficient of variation 2.5%) in the Fluosol-1% albumin perfusate during a 2-h period of recirculation in the perfusion system without a liver.

Perfusate and bile. Results obtained from three isolated livers perfused over a period of 120 min are shown in Fig. 4. When the perfusate total radioactivity data were fitted to the sum of two or three exponentials (Table III), comparison of the standard errors revealed a substantial improvement in the overall fit obtained with three as compared to two exponentials, as had already been found in intact animals. The half-life of each of these three exponentials was significantly longer than that of the corresponding exponentials in studies

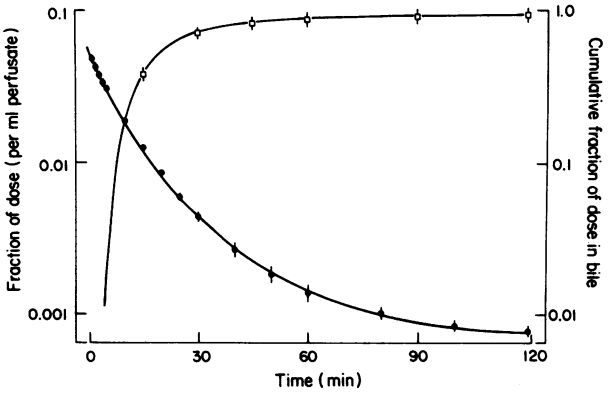

FIGURE 4 Kinetic data obtained from three isolated rat livers perfused with Fluosol-43 after pulse tracer administration of [^{3}H]bilirubin. Clearance of perfusate radioactivity (●) is expressed as a fraction of the dose per milliliter perfusate (calculated on the basis of a volume of distribution of 17 ml; see Table III) and excretion of radioactivity in bile (□) as cumulative fraction of the dose. The continuous lines represent the curves computed from the compartmental model which includes r_7 and is shown in Fig. 2.

using intact rats (Tables I and III, $P < 0.01$). Recovery of injected radioactivity in bile, 86±4% after 1 h and 90±4% after 2 h, was somewhat less (4% at 2 h) than that observed in intact animals.

Compartmental model of [^{3}H]bilirubin kinetics. Perfusate and bile data obtained from the isolated liver readily fitted the compartmental model derived using intact rats (Fig. 2). Only minor changes in the graphical presentation were necessary in order to fit the perfused liver data to the in vivo model, namely (*a*) the total simulated perfusate radioactivity concentration in l/ml (i.e. $P_n/V_n + P_u/V_u + P_c/V_c$) was compared to the experimental data, and (*b*) modification of various fractional rate constants due to the characteristics of the perfused liver system (i.e., $r_2 = 0$ assuming a negligible extravascular pool, and $r_{13} = 0$ since bilirubin degradation products were neither detectable in bile nor had any other exit route). The resulting relative accumulation of radiolabeled bilirubin degradation products in the perfusion medium may account, at least in part, for the slower disappearance of total radioactivity from perfusate than from plasma of the intact animals (Tables I and III). The fractional rate constants and distribution volumes are shown in Table II.

Radioactivity in perfusate and bile of the isolated perfused livers (Fig. 4) was compatible with the curves predicted from the intact animal model (Fig. 2, which includes r_7). Since this conformity added further support to the model-derived concept that a fraction of hepatic conjugated bilirubin is deconjugated and returned to the plasma-unconjugated bilirubin compartment, an experiment was performed to directly verify the occurrence of deconjugation.

TABLE III

*Model-independent Parameters Calculated from the Perfusate Disappearance Curve of Total ^3H-Radioactivity in Isolated Rat Liver Following [^3H]Bilirubin Administration**

Parameters†	Three exponential fit	Parameters†	Two exponential fit
A_1	0.0270±0.0041	A'_1	0.0469±0.0011
λ_1	0.162±0.019	λ'_1	0.0961±0.0025
T_1	4.29±0.49	T'_1	7.21±0.19
A_2	0.0246±0.0044	A'_2	0.00217±0.00022
λ_2	0.0693±0.0051	λ'_2	0.00894±0.00109
T_2	10.0±0.74	T'_2	77.5±9.5
A_3	0.00130±0.00014	—	—
λ_3	0.00431±0.00097	—	—
T_3	160.0±36	—	—
V	18.9±2.2		20.4±0.5
C	1.21±0.16		1.37±0.08
Standard error	2.71×10^{-5}		8.23×10^{-5}

* Data fitted to sum of two or three exponentials. To permit comparison with results obtained in intact rats (see Table I), perfusate concentration was expressed as a fraction of the administered dose per milliliter, calculated on the basis of a volume of distribution of 17 ml (approximate value calculated for intact rat of comparable size).

† See section on Data analysis and Table I for definition of symbols and units.

Deconjugation of BMG in vivo

After a tracer dose of bilirubin [^{14}C]monoglucuronide had been injected intravenously into four rats, 84±3% of the radioactivity was recovered in bile in 2 h and during the subsequent 1 h an additional 1–2% was excreted. Maximal excretion of radioactivity in bile occurred in the first 20 min after injection. In addition, 6.9±0.5% of the injected dose of radioactivity was recovered in 3 h as expired $^{14}CO_2$, reflecting metabolic degradation of the labeled glucuronic acid moiety to $^{14}CO_2$. Radiolabeled CO_2 was evident in the breath within 20 min of labeled BMG administration, reached a maximum after 40–60 min, and declined steadily during the ensuing 3 h.

DISCUSSION

Plasma radiobilirubin disappearance in intact rats and perfusate radiobilirubin disappearance in isolated perfused rat liver experiments were best described by the sum of three exponentials (Tables I and III). The initial volume of bilirubin distribution computed from the three exponentials (Table I) was comparable to the plasma volume estimated by independent methods (48). The findings are in agreement with those reported in humans (6, 8, 13) and are consistent with the prevailing concept that transport of bilirubin across the liver plasma membrane is a bidirectional process (8, 48). Experimental evidence that unconjugated bilirubin refluxes from liver to plasma has recently been obtained in studies using the radiolabeled pigment precursors δ-aminolevulinic acid (12, 13, 22), heme (49), and biliverdin (50). In the present animal experiments, an average of 20% of bilirubin entering the liver refluxed back into plasma, whereas in humans a value of 37% has been reported (8). This difference in plasma reflux is probably insufficient to account for the much faster plasma disappearance of pigment in rats ($t_{1/2}$ of initial exponential = 42 s, Table I) as compared to humans (18 min) (8). Additional factors such as species differences in albumin binding of bilirubin (51), relative liver size, and hepatic blood flow probably also play a role.

In the present experiments, a methodological problem was encountered which, while recognized previously (38, 52), has not been examined in detail in studies of bilirubin plasma disappearance and hepatic transport. Before radiobilirubin can be added to serum for injection, the crystalline pigment has to be dissolved in an aqueous solvent at alkaline pH which inevitably results in breakdown of a small amount of the pigment to labeled diazo-negative degradation products of undetermined structure (4, 38, 39). Although this can be minimized by exclusion of light and by limiting pigment exposure to the alkali to a few seconds, analysis of the injected pigment by the cetrimide extraction procedure and TLC indicated that in the present experiments an average of 6.6% of the radiobilirubin had been degraded in the process of preparing it for injection. The pigment breakdown products apparently are poorly excreted by the liver, since none

could be detected in bile and recovery of total radioactivity in bile fell 6% short of that injected. It was to be expected, therefore, that the labeled degradation products would disappear from plasma more slowly than authentic radiobilirubin. This was indeed the case, as the half-life of the terminal exponential of total radioactivity (including degraded bilirubin) was significantly longer ($P < 0.001$) than that of authentic [^{3}H]bilirubin (Table I, Fig. 3). This observation implies that in studies of bilirubin kinetics, analytical methods should be used that specifically measure radiobilirubin rather than merely extractable radioactivity. For example, in a previous investigation of plasma bilirubin kinetics in rats (20), which used a conventional solvent extraction procedure (8, 24), the half-life of the terminal exponential was disproportionately longer in relation to those of the first two exponentials than in the present study (Table I). In calculating certain model-independent parameters such as bilirubin production rate and hepatic bilirubin clearance (2, 7–10) from kinetic studies in humans, apparent slowing of the terminal exponential of plasma disappearance due to the presence of labeled bilirubin degradation products would result in substantial underestimation of the actual values. In the present studies in intact animals, we therefore expressed plasma disappearance in terms of authentic radiobilirubin rather than total radioactivity. Although the mode of elimination of the water-soluble bilirubin degradation products was not investigated, they probably are excreted preferentially in the urine (4, 38).

When the model-derived curves were applied to the experimental data obtained by analysis of plasma, liver, and bile, initial difficulties were encountered in obtaining a satisfactory fit (Fig. 3A). To achieve complete compliance, it was necessary to modify the model so that a fraction of bilirubin conjugated in the liver be deconjugated and returned to the plasma unconjugated bilirubin compartment (Figs. 2 and 3B). The occurrence of deconjugation has been verified directly by the demonstration that injected bilirubin [^{14}C]monoglucuronide is partially hydrolyzed giving rise to the appearance of $^{14}CO_2$ in expired air. Although in Fig. 2, this process of deconjugation is depicted as occurring in plasma (r_7), it is unlikely to occur at this site for the following reasons. First, no conjugated bilirubin is detectable in normal plasma (53). Second, hepatic uptake of conjugated bilirubin from plasma is more rapid than that of unconjugated pigment (21). Third, estimation of the apparent volume of distribution of the plasma conjugated bilirubin compartment (P_c) yielded an improbably high value of 166 ml (Table II). Fourth, bilirubin glucuronides added to plasma in vitro do not undergo hydrolysis (31). Thus, to resolve this apparent discrepancy in the model, a location for bilirubin deconjugation was sought which is adjacent to the plasma compartment permitting rapid equilibration with it. Since the liver was a prime candidate for this, the model was modified (Fig. 5) to include a hepatic compartment, L_{cc}, representing that fraction of conjugated bilirubin exchanging rapidly with P_c, as distinct from L_{CB} which contains conjugated bilirubin destined solely for biliary excretion. When this expanded model was tested with the experimental data, relative to the original model (Fig. 2) the fit was unchanged. Inasmuch as compartments P_c and L_{cc} could not be distinguished kinetically, it is likely that under physiological conditions P_c and L_{cc} represent a single compartment reflecting deconjugation of conjugated bilirubin in the liver with subsequent transfer of the unconjugated pigment to plasma (Fig. 5). Although by no means unique, this model is the simplest of the many examined which was compatible with all of the available data and consistent with the notion of hepatic deconjugation.

The concept that a fraction of bilirubin conjugated in the liver subsequently undergoes deconjugation is by no means novel. It was first suggested by the observation in Gunn rats that intravenous injection of normal rat bile containing conjugated bilirubin led to an increase in the plasma unconjugated pigment level (54, 55). More recently, it was found that infusion of BDG into Gunn rats resulted in biliary excretion of about 6% BMG (31). Moreover, in normal rats infused with BMG dual-labeled in the glucuronosyl and tetrapyrrole moieties, recovery in bile of the label contained in the glucuronosyl group consistently was less than that in the tetrapyrrole moiety (31). The present findings document that a major fraction of the isotope not appearing in bile is eliminated in the form of exhaled labeled CO_2. This deconjugation process appears to take place

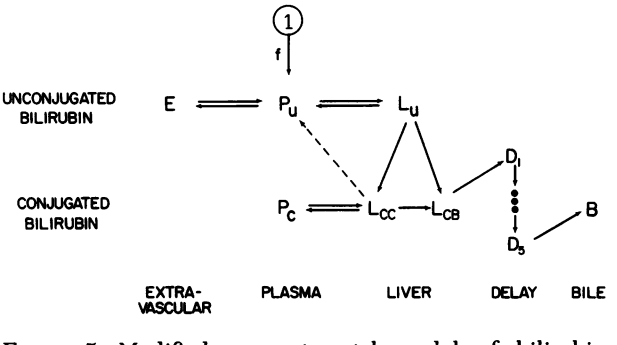

FIGURE 5 Modified compartmental model of bilirubin kinetics in the rat. See Legend to Fig. 2 for outline and definition of symbols. Compartments of the model pertaining to bilirubin degradation products have been omitted. The hepatic conjugated bilirubin compartment (L_c) has been replaced by (*a*) L_{cc} which exchanges rapidly with P_c (these two compartments are kinetically indistinguishable) and (*b*) L_{CB} which represents the hepatic conjugated bilirubin destined exclusively for biliary excretion.

largely or exclusively in the liver, as the experiments were performed in animals with an external bile fistula, thereby excluding the intestinal tract as a site of deconjugation. We have not investigated the mechanism(s) of hepatic pigment deconjugation, but have eliminated reversible transglucuronidation (i.e., 1 mol BDG + 1 mol bilirubin $\rightleftharpoons$ 2 mol BMG) as a possible mechanism by experiments in Gunn rats (31). The abundance of β-glucuronidase in the liver (56, 57) and the association of β-glucuronidase activity with bilirubin granules in cholestatic liver (54) suggest that this enzyme may be involved in the process. However, inasmuch as neither the distribution nor the transport of conjugated bilirubin in the hepatocyte are understood, the physiological role of this hydrolytic enzyme in pigment deconjugation remains conjectural.

The present findings collectively provide direct validation of the proposed compartmental model for bilirubin transport in the liver (Fig. 5). They suggest that hepatic deconjugation of a minor fraction of bilirubin glucuronides is a normally occurring metabolic event. This observation may offer a plausible explanation for the frequent occurrence of increased plasma levels of unconjugated bilirubin in patients with cholestasis (53). It further indicates that a portion of the BMG excreted in normal bile (58–61) may be derived from hydrolysis of BDG. It is possible that hepatic deconjugation is a more general mechanism, involving other endogenous substances and xenobiotics that form glucuronides. Indeed, preliminary findings with the morphine antagonist naltrexone suggest that it undergoes partial hepatic deconjugation.[3]

APPENDIX

The mathematical model corresponding to Fig. 2 is described by the following set of ordinary linear differential equations with constant coefficients:

$$\dot{P}_n = -(r_{11} + r_{13})P_n + r_{12}L_n, \quad (1)$$

$$\dot{L}_n = r_{11}P_n - r_{12}L_n, \quad (2)$$

$$\dot{E} = r_2P_u - r_1E, \quad (3)$$

$$\dot{P}_u = r_1E - (r_2 + r_3)P_u + r_4L_u + r_7P_c, \quad (4)$$

$$\dot{L}_u = r_3P_u - (r_4 + r_8)L_u, \quad (5)$$

$$\dot{P}_c = r_6L_c - (r_5 + r_7)P_c, \quad (6)$$

$$\dot{L}_c = r_8L_u - (r_6 + r_9)L_c + r_5P_c, \quad (7)$$

$$\dot{D}_1 = r_9L_c - r_{10}D_1, \quad (8)$$

$$\vdots$$

$$\dot{D}_5 = r_{10}(D_4 - D_5), \quad (9)$$

$$\dot{B} = r_{10}D_5, \quad (10)$$

with the initial conditions:

$$P_n(0) = 1 - f \quad (11)$$

$$P_u(0) = f \quad (12)$$

and all others zero initial conditions. Entities designated by capital letters are total fractional amounts in the appropriate compartments.

[3] V. Ličko. Unpublished observation.

ACKNOWLEDGMENTS

This study was supported by National Institutes of Health research grants AM-21899, AM-11275, and P50 AM-18520. We are indebted to Ms. D. Fedorchak for valuable editorial assistance. The authors also wish to express their gratitude to Dr. Colin Berry, Chesham, England for allowing us to use his method for extraction of bile pigments before publication.

REFERENCES

1. Gollan, J., L. Hammaker, V. Licko, N. Blanckaert, and R. Schmid. 1979. Hepatic deconjugation of bilirubin glucuronides: a normal metabolic pathway. *Gastroenterology.* **77:** A14 (Abstr.)
2. Carson, E. R., and E. A. Jones. 1979. Use of kinetic analysis and mathematical modeling in the study of metabolic pathways in vivo. Applications to hepatic organic anion metabolism. *N. Engl. J. Med.* **300:** 1016–1027.
3. Billing, B. H., R. Williams, and T. G. Richards. 1964. Defects in hepatic transport of bilirubin in congenital hyperbilirubinaemia: an analysis of plasma bilirubin disappearance curves. *Clin. Sci.* **27:** 245–257.
4. Ostrow, J. D., L. Hammaker, and R. Schmid. 1961. The preparation of crystalline bilirubin-C^{14}. *J. Clin. Invest.* **40:** 1442–1452.
5. Barrett, P. V. D., F. X. Mullins, and N. I. Berlin. 1966. Studies on the biosynthetic production of bilirubin-C^{14}. An improved method utilizing δ-amino-levulinic acid-4-^{14}C in dogs. *J. Lab. Clin. Med.* **68:** 905–912.
6. Araki, Y., and M. Kashima. 1968. Mathematical analysis of bilirubin dynamics in man. *In* Ikterus. K. Beck, editor. F. K. Schattauer, Verlag, Stuttgart, W. Germany. 35–45.
7. Barrett, P. V. D., P. D. Berk, M. Menken, and N. I. Berlin. 1968. Bilirubin turnover studies in normal and pathologic states using bilirubin-^{14}C. *Ann. Int. Med.* **68:** 355–377.
8. Berk, P. D., R. B. Howe, J. R. Bloomer, and N. I. Berlin. 1969. Studies of bilirubin kinetics in normal adults. *J. Clin. Invest.* **48:** 2176–2190.
9. Bloomer, J. R., P. D. Berk, R. B. Howe, and N. I. Berlin. 1971. Interpretation of plasma bilirubin levels based on studies with radioactive bilirubin. *(JAMA) J. Am. Med. Assoc.* **218:** 216–220.
10. Berk, P. D., J. R. Bloomer, R. B. Howe, T. F. Blaschke, and N. I. Berlin. 1972. Bilirubin production as a measure of red cell life span. *J. Lab. Clin. Med.* **79:** 364–378.
11. Owens, D., E. A. Jones, and E. R. Carson. 1977. Studies on the kinetics of unconjugated [^{14}C]bilirubin metabolism in normal subjects and patients with compensated cirrhosis. *Clin. Sci. Mol. Med.* **52:** 555–570.
12. Jones, E. A., R. Shrager, J. R. Bloomer, P. D. Berk, R. B. Howe, and N. I. Berlin. 1972. Quantitative studies of the delivery of hepatic synthesized bilirubin to plasma utilizing δ-aminolevulinic acid-4-^{14}C and bilirubin-^{3}H in man. *J. Clin. Invest.* **51:** 2450–2458.
13. Kirshenbaum, G., D. M. Shames, and R. Schmid. 1976. An expanded model of bilirubin kinetics: effect of feeding, fasting, and phenobarbital in Gilbert's syndrome. *J. Pharmacokinet. Biopharm.* **4:** 115–155.
14. Jones, E. A., J. R. Bloomer, P. D. Berk, E. R. Carson, D.

Owens, and N. I. Berlin. 1977. Quantitation of hepatic bilirubin synthesis in man. *In* The Chemistry and Physiology of Bile Pigments. P. D. Berk and N. I. Berlin, editors. Department of Health, Education and Welfare Publication No. (National Institutes of Health) 77-1100, Government Printing Office, Washington, D. C. 189–205.
15. Berk, P. D., J. R. Bloomer, R. B. Howe, and N. I. Berlin. 1970. Constitutional hepatic dysfunction (Gilbert's syndrome). A new definition based on kinetic studies with unconjugated radiobilirubin. *Am. J. Med.* **49:** 296–305.
16. Bloomer, J. R., P. D. Berk, R. B. Howe, and N. I. Berlin. 1971. Bilirubin metabolism in congenital nonhemolytic jaundice. *Pediatr. Res.* **5:** 256–264.
17. Frezza, M., G. Perona, R. Corrocher, R. Cellerino, M. A. Bassetto, and G. De Sandre. 1973. Bilirubin-^{3}H kinetic studies: pattern of normals, Gilbert's syndrome and hemolytic states. *Acta Hepato-Gastroenterol.* **20:** 363–371.
18. Black, M., J. Fevery, D. Parker, J. Jacobsen, B. H. Billing, and E. R. Carson. 1974. Effect of phenobarbitone on plasma [^{14}C]bilirubin clearance in patients with unconjugated hyperbilirubinaemia. *Clin. Sci. Mol. Med.* **46:** 1–17.
19. Berk, P. D., B. F. Scharschmidt, J. G. Waggoner, and S. C. White. 1976. The effect of repeated phlebotomy on bilirubin turnover, bilirubin clearance and unconjugated hyperbilirubinemia in the Crigler-Najjar syndrome and the jaundiced Gunn rat: application of computers to experimental design. *Clin. Sci. Mol. Med.* **50:** 333–348.
20. Scharschmidt, B. F., P. D. Berk, and J. G. Waggoner. 1973. Bilirubin (BR) kinetics in the normal rat. *Clin. Res.* **21:** 523. (Abstr.)
21. Shupeck, M., A. W. Wolkoff, B. F. Scharschmidt, J. G. Waggoner, and P. D. Berk. 1978. Studies on the kinetics of purified conjugated bilirubin-^{3}H in the rat. *Am. J. Gastroenterol.* **70:** 259–264.
22. Anwer, M. S., and R. Gronwall. 1976. A compartmental model for bilirubin kinetics in isolated perfused rat liver. *Can. J. Physiol. Pharmacol.* **54:** 277–286.
23. Glaser, W., W. D. Gibbs, and G. A. Andrews. 1959. The mechanism of removal of rose bengal from the plasma of the rat. *J. Lab. Clin. Med.* **54:** 556–561.
24. Weber, A. Ph., and L. Schalm. 1962. Quantitative separation and determination of bilirubin and conjugated bilirubin in human serum. *Clin. Chim. Acta.* **7:** 805–810.
25. Wolkoff, A. W., J. N. Ketley, J. G. Waggoner, P. D. Berk, and W. B. Jakoby. 1978. Hepatic accumulation and intracellular binding of conjugated bilirubin. *J. Clin. Invest.* **61:** 142–149.
26. Perrelli, W. V., and C. J. Watson. 1970. Comparison of the Weber-Schalm method with the Ducci-Watson modification of the Malloy-Evelyn method for serum bilirubin determination. *Clin. Chem.* **16:** 239–246.
27. Broderson, R. 1972. Localization of bilirubin pools in the non-jaundiced rat, with a note on bilirubin dynamics in normal human adults and in Gilbert's syndrome. *Scand. J. Clin. Lab. Invest.* **30:** 95–106.
28. Ostrow, J. D., and S. T. Boonyapisit. 1978. Inaccuracies in measurement of conjugated and unconjugated bilirubin in bile with ethyl anthranilate diazo and solvent-partition methods. *Biochem. J.* **173:** 263–267.
29. McDonagh, A. F., and F. Assisi. 1972. The ready isomerization of bilirubin IX-α in aqueous solution. *Biochem. J.* **129:** 797–800.
30. Blanckaert, N., F. Compernolle, P. Leroy, R. Van Houtte, J. Fevery, and K. P. M. Heirwegh. 1978. The fate of bilirubin-IXα glucuronide in cholestasis and during storage in vitro: intramolecular rearrangement to positional isomers of glucuronic acid. *Biochem. J.* **171:** 203–214.
31. Blanckaert, N., J. L. Gollan, and R. Schmid. 1980. Mechanism of bilirubin diglucuronide formation in intact rats. *J. Clin. Invest.* **65:** 1332–1342.
32. Blanckaert, N., J. Gollan, and R. Schmid. 1979. Bilirubin diglucuronide synthesis by a UDP-glucuronic acid-dependent enzyme system in rat liver microsomes. *Proc. Natl. Acad. Sci. (U. S. A.)* **76:** 2037–2041.
33. Hamilton, R. L., M. N. Berry, M. C. Williams, and E. M. Severinghaus. 1974. A simple and inexpensive membrane "lung" for small organ perfusion. *J. Lipid Res.* **15:** 182–186.
34. Hems, R., B. D. Ross, M. N. Berry, and H. A. Krebs. 1966. Gluconeogenesis in the perfused rat liver. *Biochem. J.* **101:** 284–292.
35. Dawson, R. M. C., and W. H. Elliott. 1959. *In* Data for Biochemical Research. R. M. C. Dawson, D. C. Elliott, W. H. Elliott, and K. M. Jones, editors. Clarendon Press, Oxford. 208.
36. Ross, B. D. 1972. Perfusion techniques in biochemistry. Clarendon Press, Oxford. 199.
37. McDonagh, A. F., and F. Assisi. 1971. Commercial bilirubin: a trinity of isomers. *FEBS (Fed. Eur. Biochem. Soc.) Lett.* **18:** 315–317.
38. Ostrow, J. D., R. Schmid, and D. Samuelson. 1963. The protein-binding of ^{14}C-bilirubin in human and murine serum. *J. Clin. Invest.* **42:** 1286–1299.
39. Lightner, D. A., A. Cu, A. F. McDonagh, and L. A. Palma. 1976. On the autoxidation of bilirubin. *Biochem. Biophys. Res. Commun.* **69:** 648–657.
40. Dixon, W. J. 1974. *In* BMD Biomedical programs (program BMD07RT). University of California Press, Berkeley, Calif. 387–396.
41. Simon, W. 1972. *In* Mathematical Techniques for Physiology and Medicine. Academic Press, Inc., New York. 112–126.
42. Mayes, P. A. 1979. Metabolism of carbohydrate. *In* Review of Physiological Chemistry. H. A. Harper, V. W. Rodwell, and P. A. Mayes, editors. Lange Medical Publications, Los Altos, California. 294–320.
43. Landaw, S. A., E. W. Callahan, and R. Schmid. 1970. Catabolism of heme in vivo: comparison of the simultaneous production of bilirubin and carbon monoxide. *J. Clin. Invest.* **49:** 914–925.
44. Lester, R., and P. D. Klein. 1966. Bile pigment excretion: a comparison of the biliary excretion of bilirubin and bilirubin derivatives. *J. Clin. Invest.* **45:** 1839–1846.
45. Blanckaert, N., K. P. M. Heirwegh, and Z. Zaman. 1977. Comparison of the biliary excretion of the four isomers of bilirubin-IX in Wistar and homozygous Gunn rats. *Biochem. J.* **164:** 229–236.
46. Lester, R., and R. Schmid. 1963. Intestinal absorption of bile pigments. I. The enterohepatic circulation of bilirubin in the rat. *J. Clin. Invest.* **42:** 736–746.
47. Lester, R., and R. Schmid. 1963. Intestinal absorption of bile pigments. II. Bilirubin absorption in man. *N. Engl. J. Med.* **269:** 178–182.
48. Scharschmidt, B. F., J. G. Waggoner, and P. D. Berk. 1975. Hepatic organic anion uptake in the rat. *J. Clin. Invest.* **56:** 1280–1292.
49. Farrell, G. C., J. L. Gollan, and R. Schmid. 1980. Efflux of bilirubin into plasma following hepatic degradation of exogenous heme. *Proc. Soc. Exp. Biol. Med.* **163:** 504–509.
50. Gollan, J. L., A. F. McDonagh, and R. Schmid. 1977. Biliverdin IXα: a new probe of hepatic bilirubin metabolism. *Gastroenterology.* **72:** 1186. (Abstr.)
51. Schmid, R., I. Diamond, L. Hammaker, and C. B. Gundersen. 1965. Interaction of bilirubin with albumin. *Nature (Lond.).* **206:** 1041–1043.
52. Schmid, R., and L. Hammaker. 1963. Metabolism and dis-

position of C^{14}-bilirubin in congenital nonhemolytic jaundice. *J. Clin. Invest.* **42**: 1720–1734.
53. Blanckaert, N., P. M. Kabra, F. A. Farina, B. E. Stafford, L. J. Marton, and R. Schmid. 1980. Measurement of bilirubin and its mono- and diconjugates in human serum by alkaline methanolysis and high-performance liquid chromatography. *J. Lab. Clin. Med.* **96**: 198–212.
54. Acocella, G., L. T. Tenconi, R. Armas-Merino, S. Raia, and B. H. Billing. 1968. Does deconjugation of bilirubin glucuronide occur in obstructive jaundice? *Lancet.* **I**: 68–69.
55. Okolicsanyi, L., P. Mangenat, and J. Frei. 1968. Deconjugation of bilirubin glucuronide by the liver. *Lancet.* **I**: 1173–1174.
56. Fishman, W. H., and A. J. Anlyan. 1947. β-Glucuronidase activity in human tissues. Some correlations with processes of malignant growth and with the physiology of reproduction. *Cancer Res.* **7**: 808–817.
57. Musa, B. U., R. P. Coe, and U. S. Seal. 1965. Purification and properties of human liver β-glucuronidase. *J. Biol. Chem.* **240**: 2811–2816.
58. Jansen, F. H., and B. H. Billing. 1971. The identification of monoconjugates of bilirubin in bile as amide derivatives. *Biochem. J.* **125**: 917–919.
59. Fevery, J., B. Van Damme, R. Michiels, J. De Groote, and K. P. M. Heirwegh. 1972. Bilirubin conjugates in bile of man and rat in the normal state and in liver disease. *J. Clin. Invest.* **51**: 2482–2492.
60. Gordon, E. R., T-H. Chan, K. Samodai, and C. A. Goresky. 1977. The isolation and further characterization of the bilirubin tetrapyrroles in bile-containing human duodenal juice and dog gall-bladder bile. *Biochem. J.* **167**: 1–8.
61. Blanckaert, N. 1980. Analysis of bilirubin and bilirubin mono- and diconjugates. Determination of their relative amounts in biological samples. *Biochem. J.* **185**: 115–128.